# Quantum physics in quantum rings

*Thomas Ihn, Andreas Fuhrer, Lorenz Meier, Martin Sigrist, and Klaus Ensslin*
*Solid State Physics, ETH Zürich • 8093 Zürich, Switzerland*

The symmetry of a ring system is crucial for classical and quantum effects. Mathematically speaking a ring is a non-singly connected geometry. In quantum mechanics the ring symmetry of the benzene molecule gives rise to its delocalized electronic states [1]. In ring geometries strongly connected to external leads the electron wave packets can take two different paths around the ring which gives rise to interference. This is reminiscent of Young's double-slit experiment for photons. The use of charged particles in a ring geometry rather than neutral photons allows the relative phase of the electronic wave function in the two arms of the ring to be manipulated by a magnetic field perpendicular to the plane of the ring. Aharonov and Bohm proposed such a set-up to test experimentally the significance of the magnetic vector potential in quantum mechanics [2]. They predicted that the phase difference of the alternative paths changes by $2\pi$ as the flux through the ring is changed by one flux quantum h/q (q is the charge of the particle). Many experiments over the last three decades have demonstrated magnetic field periodic resistance oscillations in ring structures with a phase coherence length longer than or comparable to the perimeter. In mesoscopic physics the Aharonov-Bohm (AB) effect has become a standard tool to quantitatively investigate the phase coherence of transport in metallic [3] and semiconducting systems.

In closed systems with fixed electron number a characteristic magnetic flux-periodic energy spectrum evolves. Such a spectrum can be detected experimentally by measuring electron transport through a lithographically defined quantum ring in the Coulomb blockade regime.

In ring-shaped confined quantum systems the angular momentum becomes a good quantum number. In the case of a single mode ring the single-particle energy levels are given by:

$$E_{m,l} = \frac{\hbar^2}{2m^* r^2}(m\text{-}l)^2$$

Here $l$ is the angular momentum quantum number and m is the magnetic quantum number, i.e. the number of flux quanta penetrating the ring at a given external magnetic field. The only material-dependent parameter is the effective mass, $m^*$. The ring radius is denoted by $r$. At zero magnetic field, $m = 0$, the ground state has angular momentum $l = 0$, the next two degenerate states are characterized by $l = \pm 1$ and so forth. At finite magnetic field the ground state develops a finite angular momentum which can be translated into a persistent current [4]. In this model the wave functions are plane waves extended around the ring independent of magnetic field.

## Fabrication of quantum rings

In this article we describe recent experiments on quantum rings realized in semiconductor heterostructures. Figure 1 shows the

### Aharonov-Bohm effect

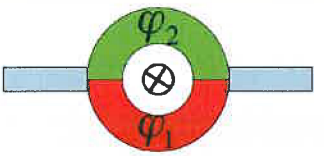


$$\Delta\varphi = \varphi_1 - \varphi_2 = \varphi_{geom.} + \frac{q}{h}\oint \vec{A}d\vec{l}$$

An electron wave coming from the left travels through the ring. The wave propagates in the upper as well as in the lower arm and interferes with itself. The phase accumulation in the upper arm is φ1, in the lower arm φ2. The phase difference Δφ is determined by a constant depending on the details of the wave propagation in the two arms ($\varphi_{geom}$) and the magnetic flux penetrating the ring. In the above equation the vector potential in the ring has to be integrated over the ring circumference, q is the particle's charge. As the flux through the ring is changed by one flux quantum q/h, the phase difference changes by $2\pi$. Therefore the interference condition, be it constructive, destructive or in between, becomes periodic in the magnetic flux penetrating the ring. Destructive interference corresponds to a low conductance of the ring, constructive interference to a high conductance. Consequently the conductance of the ring oscillates periodically with magnetic field. All of the above statements are correct if the phase coherence length of the electrons is at least as long as the circumference of the ring.

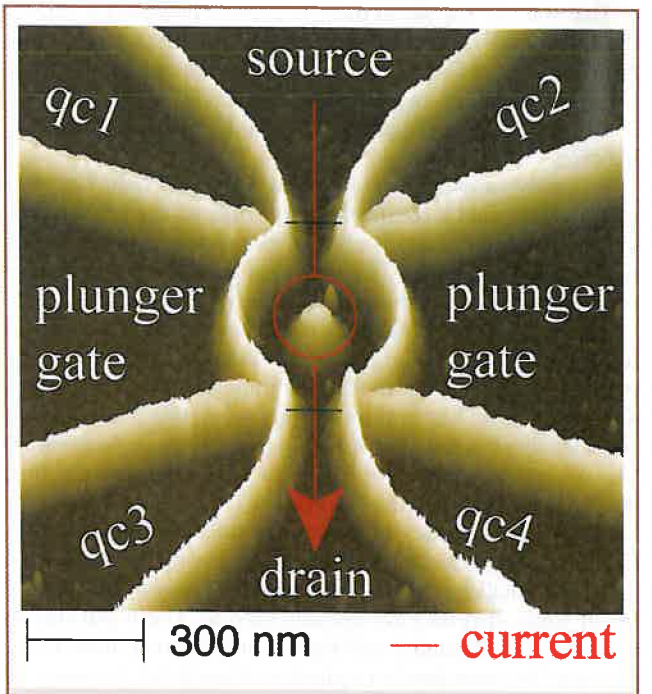


▲ **Fig. 1:** Micrograph of the quantum ring. The red line marks the current flow from source to drain through the two quantum point contacts and the ring. The lateral gate electrodes termed qc1-qc4 are used to tune the tunnel barriers (indicated by dotted lines) connecting the quantum ring to its leads. The plunger gates allow the electron number on the ring to be controlled (adapted from Ref. 5).

topography of a GaAs-AlGaAs heterostructure containing a two-dimensional electron gas below the surface.
The bright lines are patterned by local oxidation with a voltage-biased tip in a humid environment. The electron gas is depleted below the oxide lines. Voltages applied across oxide lines separating brown regions containing highly mobile electrons do not lead to detectable levels of current flow. Such biased areas can therefore be used as lateral gates to adjust electrical potentials between these regions. The current flowing from source to drain indicated by the red line has to pass between a first constriction, called a quantum point contact (QPC see black dotted lines in Fig. 1), then takes the two possible paths in the ring and leaves again through a QPC constriction. The QPC constrictions can be tuned into the tunneling regime by appropriate voltages applied to the lateral gates termed "qc1-qc4". This way a circular quantum system is realized which is weakly coupled to source and drain reservoirs. The ring contains about 150 electrons and 2-3 radial modes are occupied. For details see Ref. 5.

## Electronic transport through quantum rings

Figure 2 shows the conductance through the quantum ring as a function of an energy scale that is deduced from the applied plunger-gate voltage by calibration. The charge on the ring is tuned in steps of the quantum of electronic charge e. Most of the time the conductance vanishes. This is called the Coulomb blockade where the energy provided by the applied voltages is not sufficient to induce another electron onto the ring. At certain voltages or energies, however, the Fermi levels in source and drain are aligned with an energy level in the quantum ring. This level arises from the energy difference of the n and (n+1) many-particle states in the ring. The fluctuating charge on the ring gives rise to the sharp conductance resonances as illustrated in Fig. 2. If temperature is sufficiently low (below 100 mK in this case) and the coupling of the ring to source and drain sufficiently weak so that the broadening of quantum states is less than their spacing then the position and height of each conductance resonance is determined by the properties of a specific quantum state.

## Energy spectrum of quantum rings

In a simple picture the change in voltage position of a conductance resonance can be identified with the change in energy of a single-particle quantum state. Figure 3 shows a conductance map of 5 such experimentally determined states and their behavior as a function of perpendicular magnetic field.

The states are separated by the energy cost to add an electron to the quantum ring. The dominant contribution is the charging energy $e^2/2C$, where C is the capacitance of the system. In addition, the single-particle confinement energy is relevant as well as possible contributions of exchange and correlation. The top two states display a zig-zag movement as predicted by the single-mode ring model presented before. The periodicity is given by one flux quantum h/e per ring area. The fact that the upper two states display similar magnetic field dispersion indicates that their orbital states are related. The behavior can be interpreted as the successive filling of one orbital state with a spin-up and a spin-down electron.

The three lower lying states also show a B-periodic pattern (see Fig. 3), but no zig-zag behavior. They arise from mixing clean angular momentum states by imperfections in the sample. For example, the presence of source and drain contacts perturbs the ring symmetry and mixes angular momentum states.

The ring spectrum therefore contains two typical kinds of states (see Fig. 4): firstly, well-defined angular momentum states

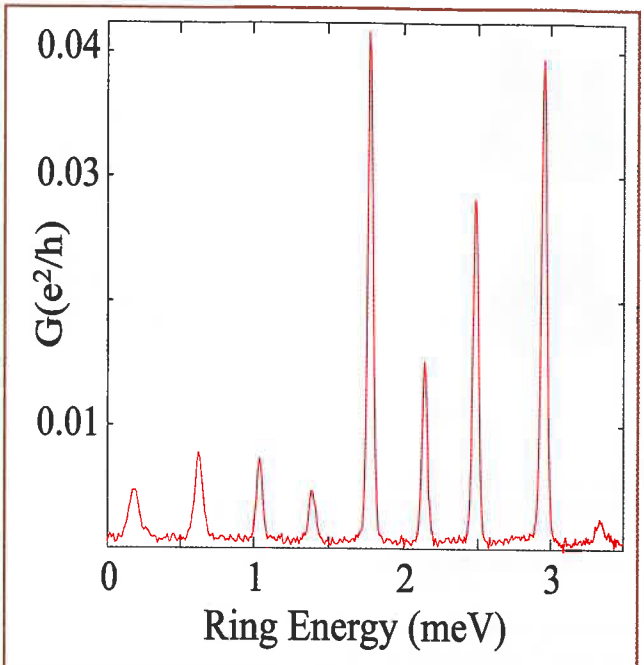


▲ **Fig. 2:** Conductance in units of the quantum conductance $e^2/h$ through the quantum ring measured by applying a small but finite bias between source and drain contacts. The energy axis is deduced from the applied lateral-gate voltage and an experimentally determined lever arm between voltage and energy.

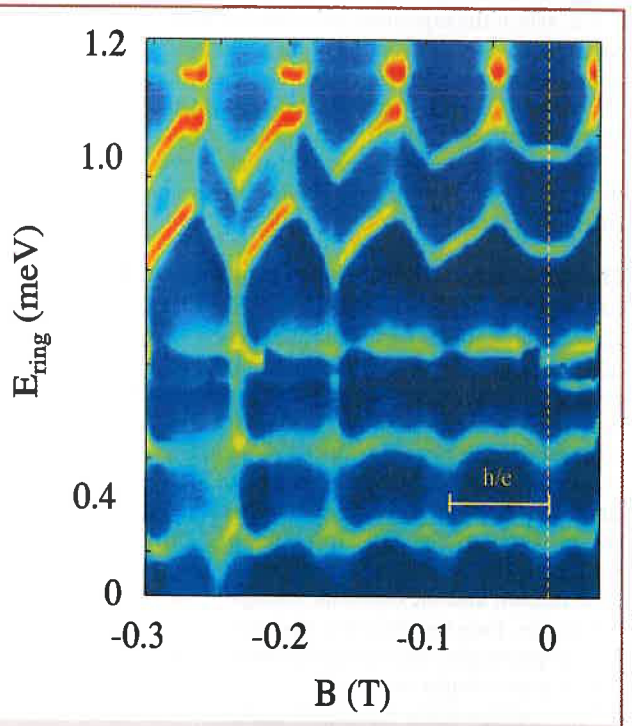


▲ **Fig. 3:** Conductance map of ring energy (gate voltage) versus perpendicular magnetic field. Blue means low conductance and yellow/red high conductance. A vertical cut at constant magnetic field displays conductance resonances similar to those shown in Fig. 2. (Adapted from Ref. 5).

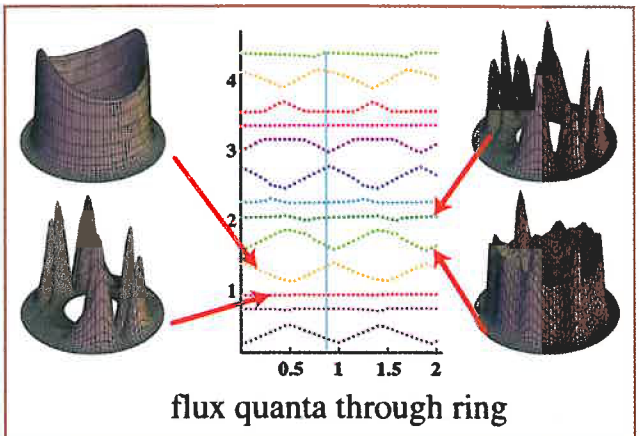


▲ Fig. 4: Calculated magnetic field dependence of energy levels in a quantum ring whose circular symmetry is perturbed. The four wave functions to the left and right are related to the energy levels as indicated by the arrows.

displaying a zig-zag magnetic field dispersion with a plane wave-like wave function extended around the ring; secondly, states containing a mixture of angular momenta with a rather flat magnetic field dispersion and a wave function which is strongly modulated (or localized) at certain locations around the ring. Such a peculiar situation is unique to ring systems, where the non-singly connected geometry plays a decisive role. From the experimental determination of the conductance resonances as a function of magnetic field one can determine the qualitative character of the corresponding wave function. The fact that about 50% of the experimentally detected quantum states display zig-zag behavior as a function of magnetic field indicates the high quality of the ring potential. The slope of such zig-zag states is directly related to their angular momentum and therefore to the persistent current contribution of these states [4]. Our findings here are in qualitative agreement with previous experiments using SQUIDs as detectors for the magnetic moment of such circulating currents.

## The spin degree of freedom in quantum rings

Given the fact that two qualitatively different types of states (with zig-zag and flat magnetic field dispersion) can be detected in quantum rings, the system can be regarded as being similar to a double dot system. A crossing between states of these two types (an unperturbed angular momentum state and a mixed angular momentum state) can be induced by a controlled application of asymmetric gate voltages. Far away from the crossing the two states are filled successively with spin-up and spin-down electrons. Close to the crossing the spin filling sequence is determined by a competition between the single-particle Hartree contribution and the exchange energy. If the exchange energy dominates, then the first two electrons filled in the two levels form a spin-triplet. For increasing Hartree contribution a transition to a spin-singlet occurs [6].

Spin configurations in coupled quantum systems are relevant in view of concepts to use the electron spin in quantum dots as a qubit for quantum information processing [7]. Singlet-triplet transitions can naturally be tuned via the application of a magnetic field, which is usually a slow process. Gate voltages can potentially be tuned very fast. In a configuration as discussed before a singlet-triplet transition can be tuned entirely by electric fields without the assistance of a magnetic field. The fact that the orbital degrees of freedom in quantum rings can be understood on a quantitative basis, can be exploited to analyze and manipulate the spin states in such systems.

Another important physical effect related to the electron spin is the Kondo effect. For quantum dots strongly coupled to their leads, correlations between an unpaired electron spin in the dot and the electrons in the leads give rise to an enhanced Kondo density of states pinned at the Fermi level between two electronic levels. In quantum dots the Kondo effect has been intensively investigated during the last 6 years (see e.g Ref. 8). The Kondo effect can also be observed in quantum rings strongly coupled to their leads [9]. The experimentally observed features related to the Kondo effect, such as a zero-bias anomaly or an enhanced conductance in the Coulomb blockade regime, appear flux-periodic in a magnetic field as in the energy spectrum discussed before. A careful analysis reveals that it is the coupling of the ring states to the leads which strongly oscillates as a function of magnetic field and therefore influences the characteristic Kondo temperature of a particular configuration. In combination with the singlet-triplet transition discussed before the Kondo effect can be investigated for various spin configurations in the ground state of the quantum ring.

## Dots and rings

The fabrication of quantum rings relies on the depletion of the electron gas at a small and well-defined spot within the nanostructure. Using an atomic force microscope (AFM) to locally oxidize and therefore deplete an electron gas is a versatile method to pattern tunable ring structures with excellent electronic properties. Figure 6 shows two other examples of ring structures connected to or even containing quantum dots. The left part [Fig. 6 (a)] shows a central ring structure whose circuit is indicated by the green line. On top and bottom two quantum dots flank the ring (red lines). Two additional circuits at the very top and bottom (blue lines) contain quantum point contacts (QPC). All five circuits can be operated separately to detect the coupling of the involved quantum structures. A QPC circuit can be tuned to the tunneling regime, where the QPC conductance is very sensitive to its environment. In this situation, each additional charge on the quantum dot changes the electrostatic

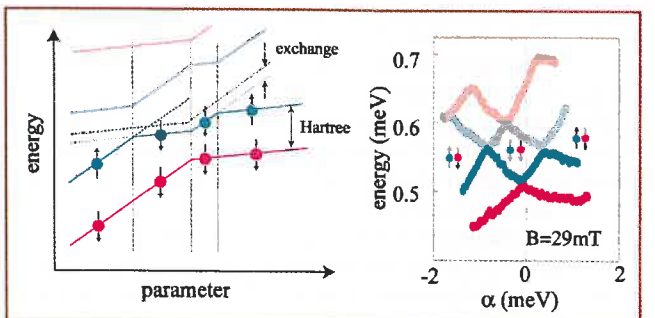


▲ Fig. 5: **(left)** Two orbital levels cross as a function of some external parameter, e.g. asymmetric gate voltage. Before and after the crossing the ground state for the lowest two electrons is a singlet state. At the anti-crossing, if exchange dominates the Hartree contribution, the spins of the lowest two electrons are aligned. **(right)** This shows an example of such a situation in our ring. The measured levels have been extracted from peak positions in conductance maps as a function of both ring energy and gate asymmetry α [6]. Between the two blue peak positions the spin state can be tuned with gate voltages.

potential in the neighboring QPC and therefore its conductance. The QPC can thus be used as a non-invasive charge detector [10] in regimes, where direct transport through the quantum dot is experimentally difficult to access. Similarly the central ring structure can be used as a charge detector of the dot [11]. Phase-coherent transport through the open ring gives rise to Aharonov-Bohm oscillations in the conductance. If the charge on the quantum dot is changed by one electron then the electrostatic potential in one arm of the ring is slightly changed. This changes the overall phase of the wave function and gives rise to a change of the total transmission through the ring, which can be detected experimentally. Such electrostatic coupling between quantum structures is important to understand their cross-talk. For future quantum circuits it will be important to couple quantum systems not just by electrostatic, but by real quantum mechanical coupling involving overlap of wave functions.

The right part in Fig. 6 (b) shows a four-terminal ring structure. Electrons injected through one of the contacts travel ballistically through the ring structure with only a small fraction leaving through the first side arm. In the ballistic phase-coherent regime Aharonov-Bohm oscillations can be observed in a usual two-terminal set-up as well as in three- and four-terminal configurations. The four gate electrodes between the ring contacts can be used to electrostatically squeeze each quadrant of the ring separately. In particular, a quantum dot can be electrostatically induced in each of the four quadrants. We have extensively studied the situation when two quantum dots (indicated by the red circles) appear in two arms of the rings, such that an electron wave packet traveling along the path indicated by the green line passes both dots if an interference signal is detected. The phase evolution of the electronic wave function has been studied experimentally [12] where one dot has been included in one arm of the Aharonov-Bohm interferometer. In the present case the two dots play an important role for the interference experiment. The phase change can be detected when an electron is added to each of the dots separately, to both dots at the same time, or when one electron is effectively transferred from one dot to the other. In many regimes we find that the phase of the electronic wave function is changed by about $\pi$ as the system goes through a conductance resonance. It is important to note, however, that every component of the system plays a role since phase coherence is maintained. Changing the electron number in one of the dots by one has an impact on the boundary condition of the wave function at several locations in the ring. The interference pattern may therefore develop complicated features which depend on the details of the system and the changes of its components. ■

## About the authors

**Thomas Ihn** received his diploma from the TU Munich and did his PhD at the Paul-Drude Institute in Berlin. He was a postdoc in Nottingham and is a senior scientist at ETH Zürich since 1999.
**Andreas Fuhrer** received his diploma and PhD from ETH Zürich and is a postdoc at Lund University since 2004.
**Lorenz Meier** received his diploma from ETH Zürich in 2003 and is working on a Phd thesis in a joint project between IBM and ETH Zürich.
**Martin Sigrist** finished his diploma in 2002 and is working on his PhD thesis at ETH Zürich.
**Klaus Ensslin** studied in Munich and Zürich, worked on his PhD at the Max-Planck Institut in Stuttgart, was a postdoc at UCSB and at the University of Munich and is a professor at ETH Zürich since 1995.

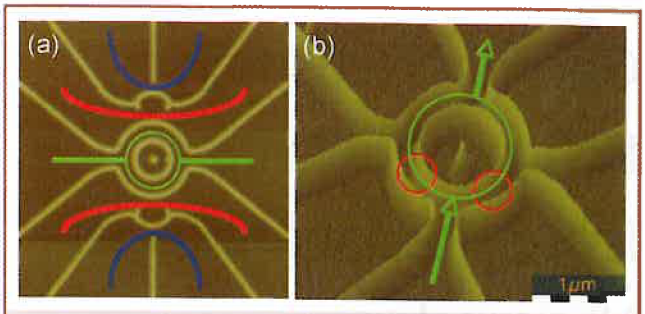


▲ **Fig. 6:** (a) AFM image of a circuit containing a central ring (current flow indicated by green line), two quantum dots (red line) and two quantum point contacts at the very top and bottom (blue line). The bright lines represent oxide lines below which the electron gas is depleted. Conductances can be measured along each of the colored lines plotted in the figure (adapted from Ref. 11).
(b) Four-terminal ring structure defined by oxide lines (bright lines) as before. By applying lateral gate voltages to the four outer segments the current paths in the ring can be electrostatically squeezed to form quantum dots. Two such possible locations of electrostatically induced quantum dots are indicated by the red circles. For current flow from bottom to top (indicated by the green line) each partial wave has to pass a quantum dot and change its phase correspondingly (adapted from Ref. 13)

## Acknowledgements

We thank many collaborators for their contribution to the results presented here. An important requirement for the fabrication of semiconductor nanostructures are high-quality heterostructures. We thank Werner Wegscheider for providing excellent material for our experiments. Financial support is acknowledged from the Swiss Science Foundation (Schweizerischer Nationalfonds).

## References

[1] Kekulé, Bull. Soc. Chim. Fr. 3, 98 (1865)
[2] Y. Aharonov and D. Bohm, Phys. Rev. 115, 485 (1959)
[3] A.G. Aronov and Y.V. Sharvin, Rev. Mod. Phys. 59, 755 (1987).
[4] M. Büttiker, Y. Imry, and R. Landauer, Phys. Lett. 96A, 365 (1983)
[5] A. Fuhrer, S. Lüscher, T. Ihn, T. Heinzel, K. Ensslin, W. Wegscheider, and M. Bichler, Nature 413, 822 (2001)
[6] A. Fuhrer, T. Ihn, K. Ensslin, W. Wegscheider, and M. Bichler , Phys. Rev. Lett. 91,206802 (2003)
[7] D. Loss and D. P. DiVincenzo, Phys. Rev. A 57, 120 (1998)
[8] D. Goldhaber-Gordon, H. Shtrikman, D. Mahalu, D. Abusch-Magder, U. Meirav, and M. A. Kastner, Nature 391, 156 (1998)
[9] A. Fuhrer, T. Ihn, K. Ensslin, W. Wegscheider, and M. Bichler, Phys. Rev. Lett. 93, 176803 (2004)
[10] M. Field, C. G. Smith, M. Pepper, D. A. Ritchie, J. E. F. Frost, G. A. C. Jones, and D. G. Hasko, Phys. Rev. Lett. 70, 1311 (1993)
[11] L. Meier, A. Fuhrer, T. Ihn, K. Ensslin, W. Wegscheider, and M. Bichler, Phys. Rev. B 69, 241302 (2004)
[12] R. Schuster, E. Buks, M. Heiblum, D. Mahalu, V. Umansky, and H. Shtrikman, Nature 385, 417 (1997).
[13] M. Sigrist, A. Fuhrer, T. Ihn, K. Ensslin, S. E. Ulloa, W. Wegscheider, and M. Bichler, Phys. Rev. Lett. 93, 66802 (2004)